

# Supporting Information for

## Fluorinated Click-Derived Tripodal Ligands Drive

### Spin Crossover in both Iron(II) and Cobalt(II)

### Complexes

*Maite Nößler,<sup>[a],⊥</sup> David Hunger,<sup>[c],⊥</sup> Nicolás I. Neuman,<sup>[a, b, f]</sup> Marc Reimann,<sup>[d]</sup> Felix Reichert,<sup>[e]</sup> Mario Winkler,<sup>[c]</sup> Johannes Klein,<sup>[a]</sup> Tobias Bens,<sup>[b]</sup> Lisa Suntrup,<sup>[a]</sup> Serhiy Demeshko,<sup>[e]</sup> Jessica Stubbe,<sup>[a]</sup> Martin Kaupp,<sup>[d]</sup> Joris van Slageren<sup>[c]\*</sup> and Biprajit Sarkar<sup>[a, b]\*</sup>*

<sup>[a]</sup>Institut für Chemie und Biochemie, Freie Universität Berlin, Fabeckstraße 34-36, D-14195, Berlin, Germany

<sup>[b]</sup> Lehrstuhl für Anorganische Koordinationschemie, Universität Stuttgart, Pfaffenwaldring 55, D-70569 Stuttgart, Germany

<sup>[c]</sup> Institut für Physikalische Chemie, Universität Stuttgart, Pfaffenwaldring 55, 70569 Stuttgart, Germany

<sup>[d]</sup> Institut für Theoretische Chemie, Technische Universität Berlin, Straße des 17. Juni 135, D-10623 Berlin, Germany

<sup>[e]</sup> Institut für Anorganische Chemie, Universität Göttingen, Tammanstraße 4, D-37077, Göttingen, Germany

<sup>[f]</sup> Instituto de Desarrollo Tecnológico para la Industria Química, INTEC, UNL-CONICET Paraje El Pozo, Santa Fe, Argentina

⊥ Equal contribution

## **Content**

Magnetometric Measurements	S1
Mössbauer Spectroscopy	S3
EPR Spectroscopy	S4
X-Ray Crystallography	S4
IR Spectroscopy	S7
NMR Spectra	S8

## Magnetometric Measurements



Figure S 1: Preparation of the samples. Top: compound in eicosan-matrix in plastic capsule. Bottom: compound ground and pressed into a pellet.

---

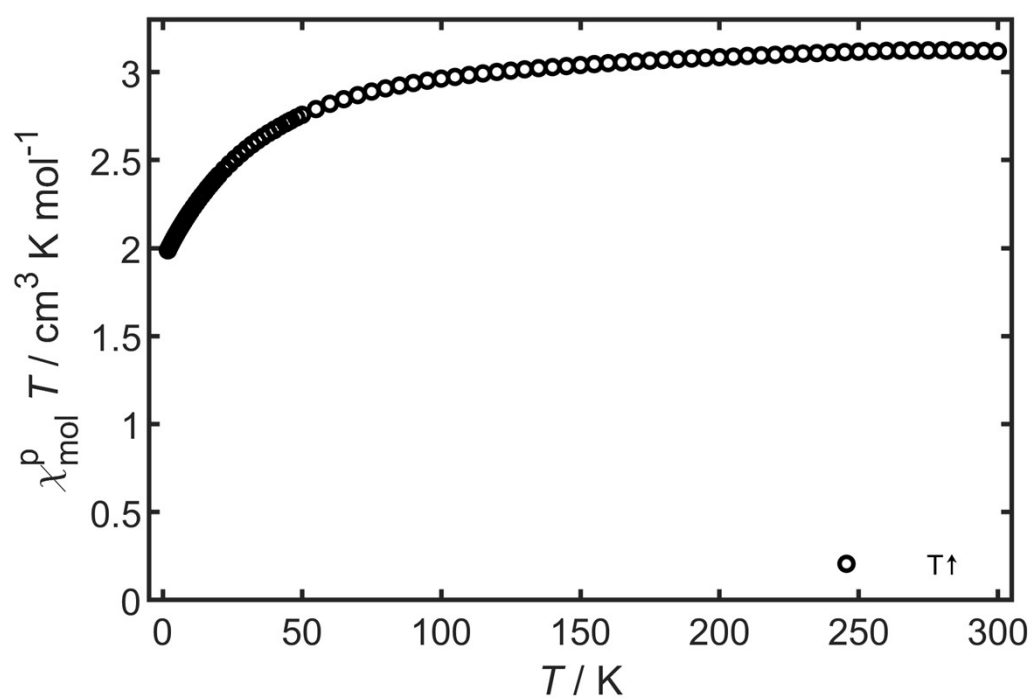


Figure S 2:  $\chi_{\text{M}}T$  vs.  $T$  of complex 1 pressed in a pellet.

---

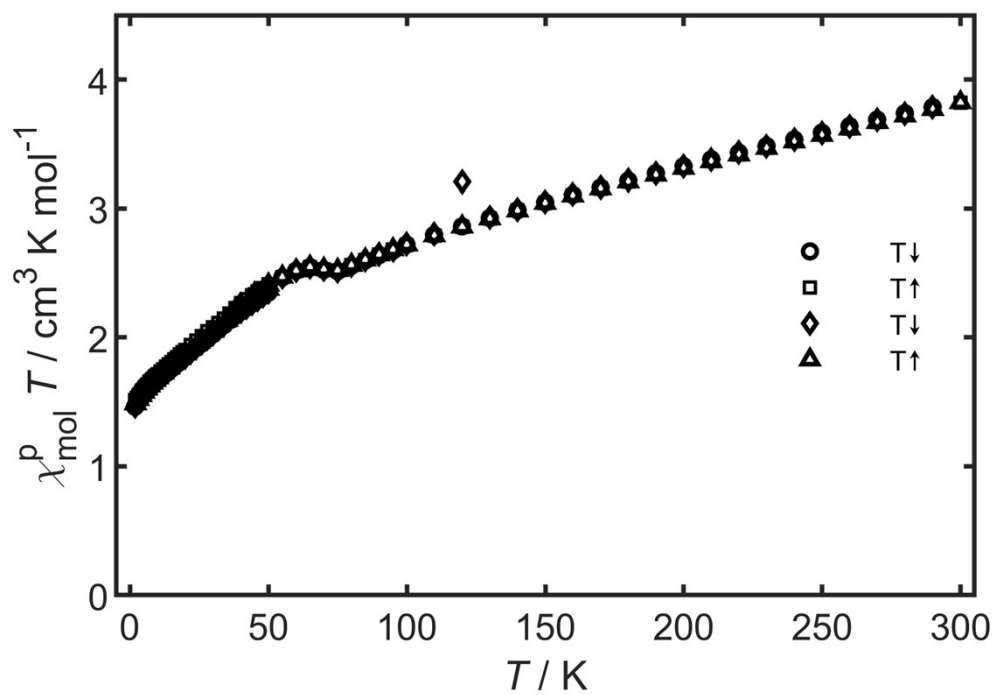


Figure S 3: Susceptibility-temperature product of complex 2 from 1.8 to 300 K. The sample was prepared in an eicosan matrix.

---

## Mössbauer Spectroscopy

Mössbauer spectra at 80 and 292 K were recorded for Complex **3**.

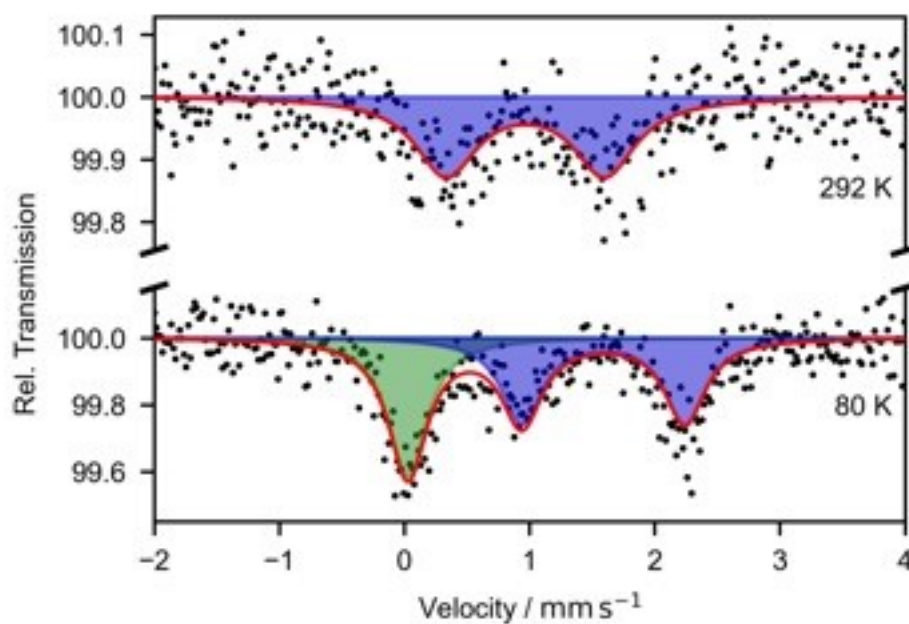


Figure S4: Mössbauer spectra of complex **3** at the indicated temperatures. Measurements were done on the same sample as in the case of the magnetometry. Fits are shown as red solid lines. The contribution of each spin species is shown in green (low spin) and blue (high spin).

Table S1: Overview of the fit parameters from the temperature dependent Mössbauer measurements of **3**.

System		80 K	292 K
<b>S = 2</b>	$\delta_{IS} / \text{mm s}^{-1}$	1.59(1)	0.97(1)
	$\Delta E_{QS} / \text{mm s}^{-1}$	1.30(1)	1.27(1)
	$\Gamma / \text{mm s}^{-1}$	0.40(1)	0.60(1)
<b>S = 0</b>	$\delta_{IS} / \text{mm s}^{-1}$	0.03(1)	-
	$\Gamma / \text{mm s}^{-1}$	0.38(1)	-
<b>HS molar fraction</b>		0.56	1

## EPR Spectroscopy

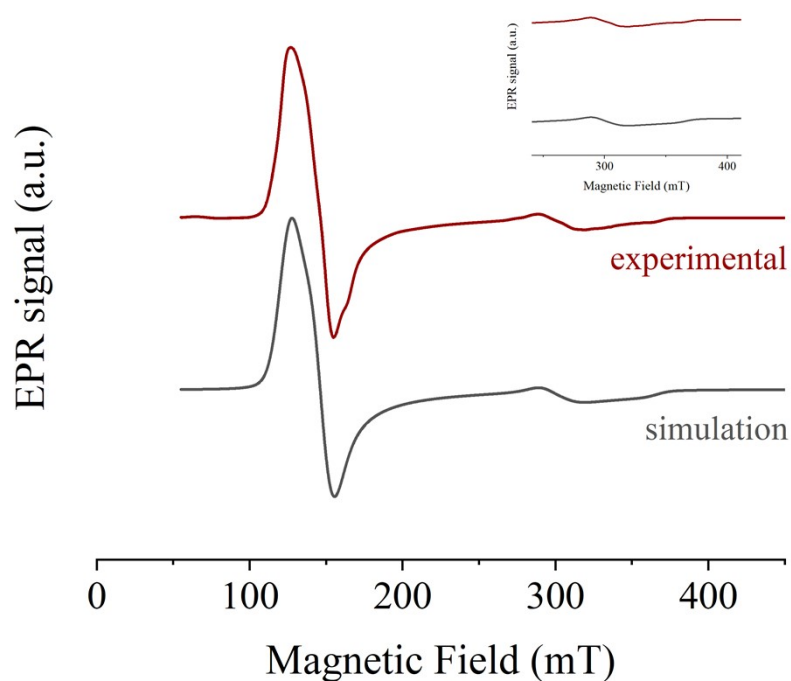


Figure S5: EPR Spectrum of **2** at 13K.

## X-Ray Crystallography

Table S2: Crystallographic data of **1**, **2** and **3**.

	<b>1</b>	<b>2</b>	<b>3</b>
Chemical formula	$C_{62}H_{62}B_2CoF_{14}N_{20}O_2$	$C_{60}H_{54}B_2CoF_{14}N_{20}$	$C_{62}H_{53}B_2CoF_{14}N_{20}O$
$M_r$	1465.86	1401.78	1437.71
Crystal system	Monoclinic	Triclinic	Monoclinic
Space group	$P2_1/n$	$P-1$	$P2_1/n$
a (Å)	7.7391(3)	14.384(6)	7.8403(4)
b (Å)	20.7813(8)	14.984(6)	20.397(1)
c (Å)	20.1509(9)	15.384(6)	19.7649(9)
$\alpha$ (°)	90	91.16(1)	90
$\beta$ (°)	98.408(3)	107.86(1)	97.184(2)
$\gamma$ (°)	90	93.21(1)	90
V (Å <sup>3</sup> )	3206.0(2)	3148(2)	3136.0(3)
Z	2	2	2
Density (g cm <sup>-3</sup> )	1.518	1.479	1.523
F(000)	1506	1434	1470

Radiation Type	MoK $_{\alpha}$	MoK $_{\alpha}$	MoK $_{\alpha}$
$\mu$ (mm $^{-1}$ )	3.003	0.372	0.344
Crystal size	0.18 x 0.08 x 0.08	0.14 x 0.13 x .0.1	0.08x0.06x0.02
Meas. Refl.	21514	38191	89633
Indep. Refl.	5786	11473	5774
Obsvd. [ $I > 2\sigma(I)$ ] refl.	4420	7519	5036
R $_{\text{int}}$	0.0634	0.0602	0.0725
R [ $F^2 > 2\sigma(F^2)$ ], wR( $F^2$ ), S	0.0928, 0.2274, 1.094	0.0597, 0.1607, 1.066	0.0655, 0.1679, 1.130
$\Delta\rho_{\text{max}}$ , $\Delta\rho_{\text{min}}$ (e $\text{\AA}^{-3}$ )	0.882, -0.660	0.644, -0.543	0.537, -1.058

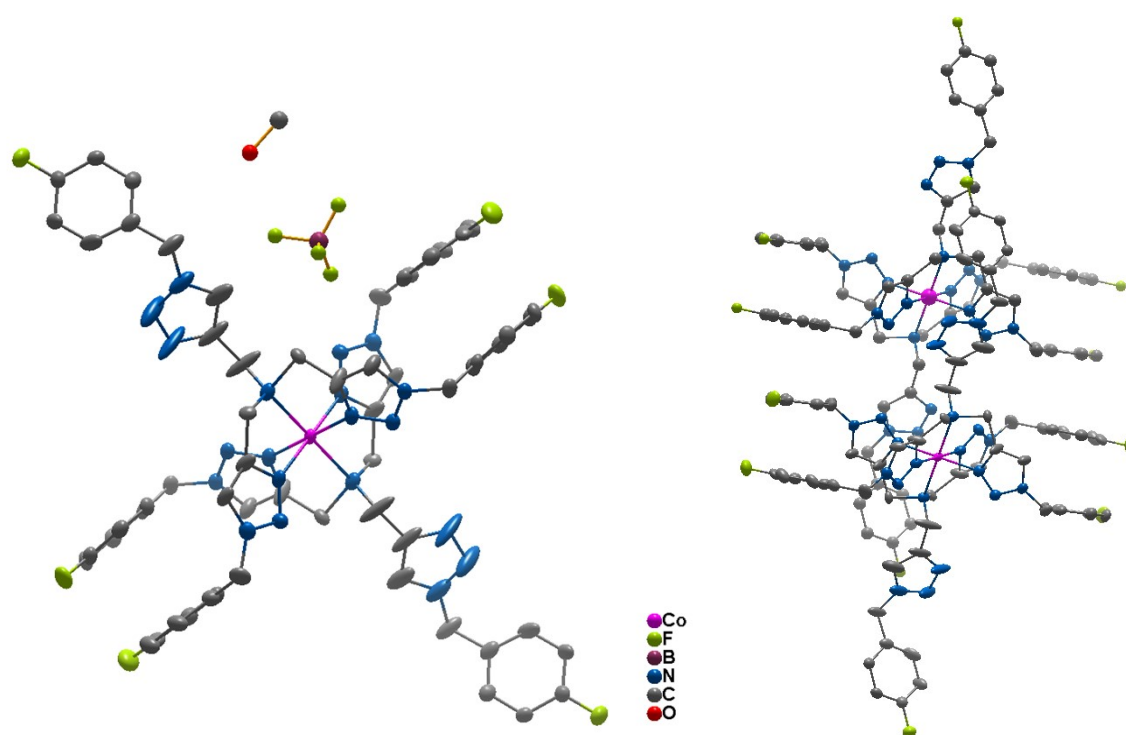


Figure S6: Perspective view of **1**, left with solvent molecule and anion, right: stacking of two molecules. Ellipsoids are at a probability level of 50%. H atoms, anions and solvent molecules are omitted for clarity.

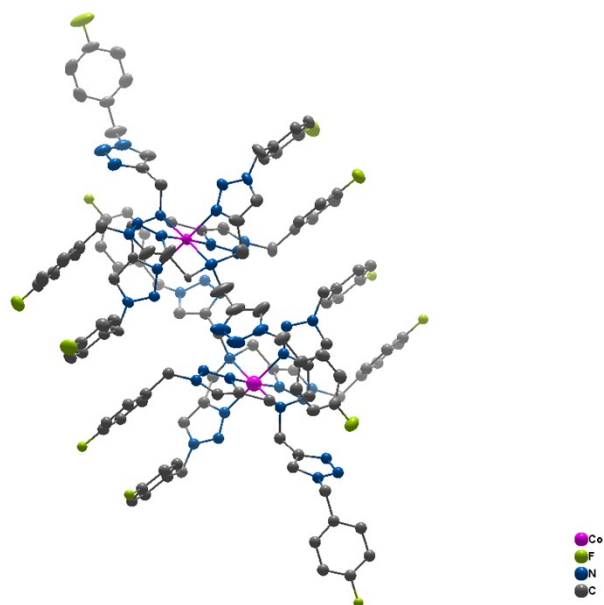


Figure S7: Perspective view of **2**, stacking of two molecules. Ellipsoids are at a probability level of 50%. H atoms, anions and solvent molecules are omitted for clarity.

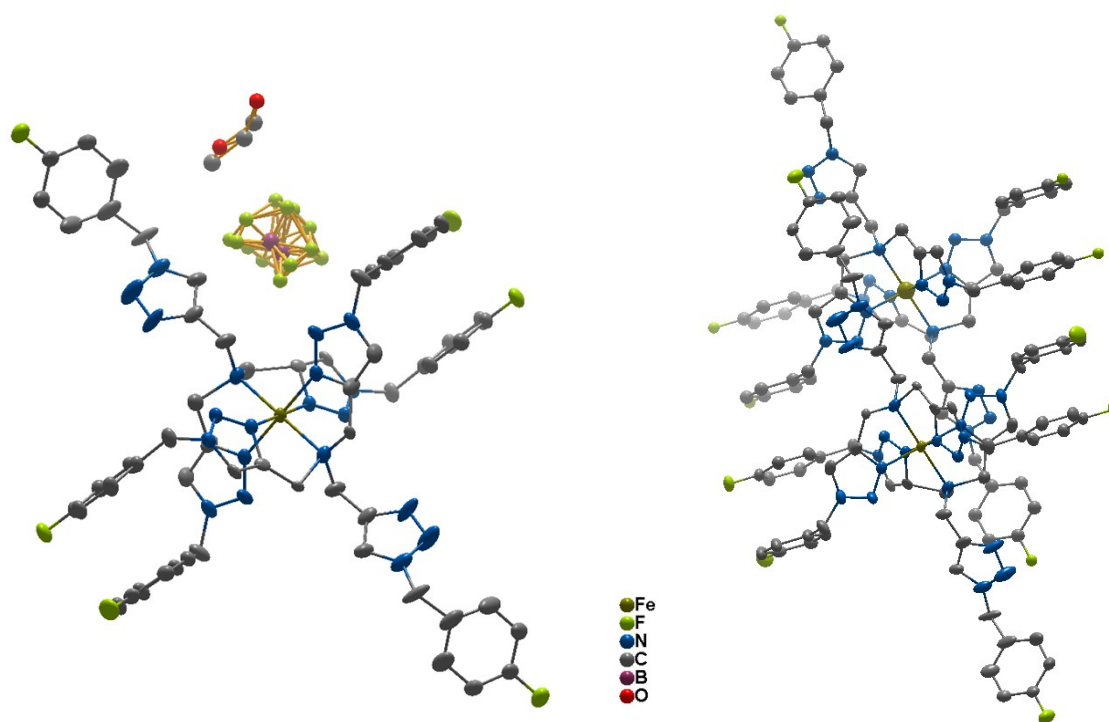


Figure S8: Perspective view of **3**, left with solvent molecule and anion, right: stacking of two molecules. Ellipsoids are at a probability level of 50%. H atoms, anions and solvent molecules are omitted for clarity.



## IR Spectroscopy

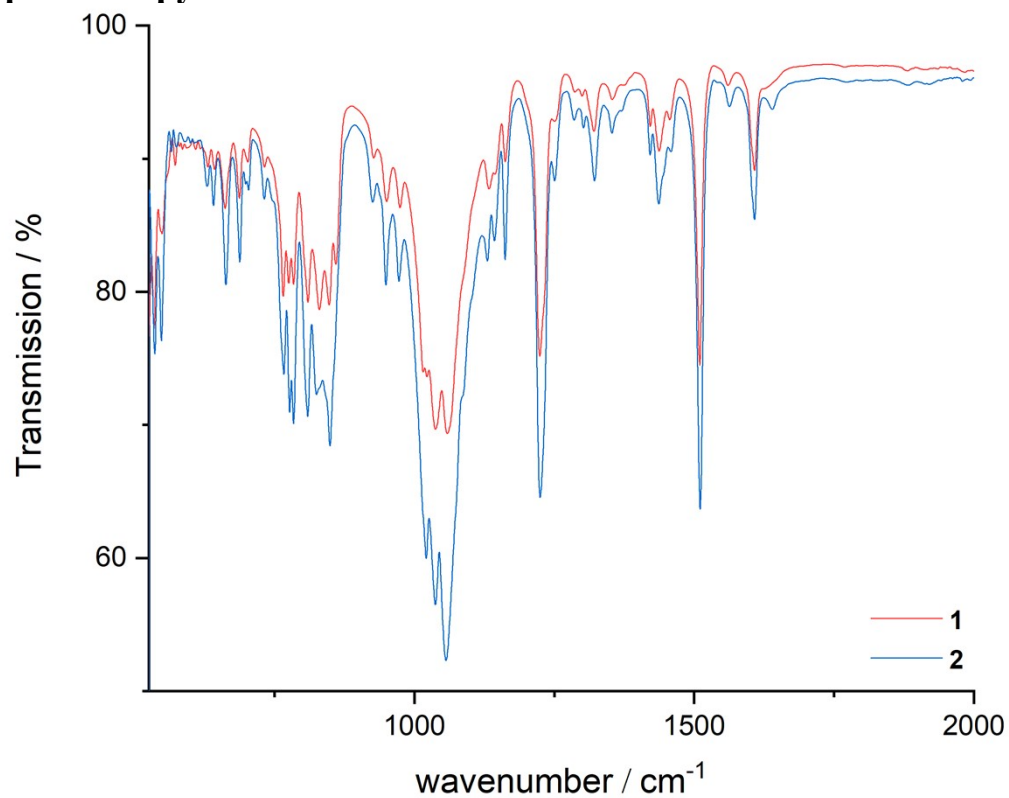


Figure S 9: IR spectra of **1** and **2**.

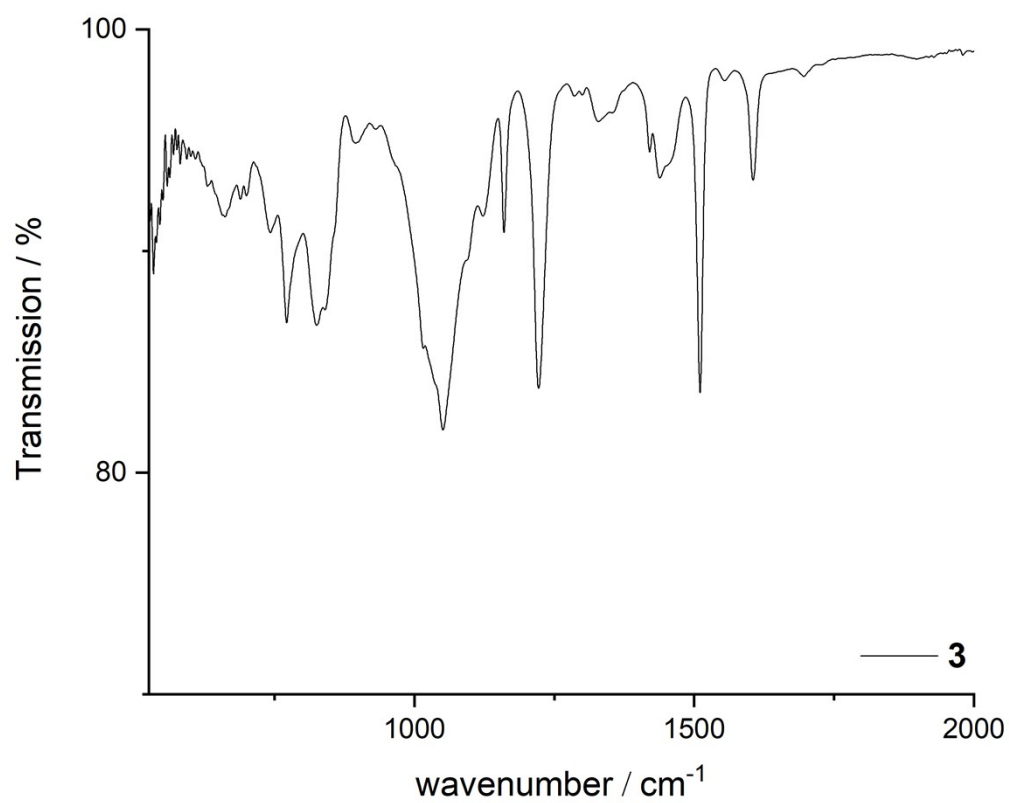


Figure S 10: IR spectrum of **3**.

# NMR Spectra

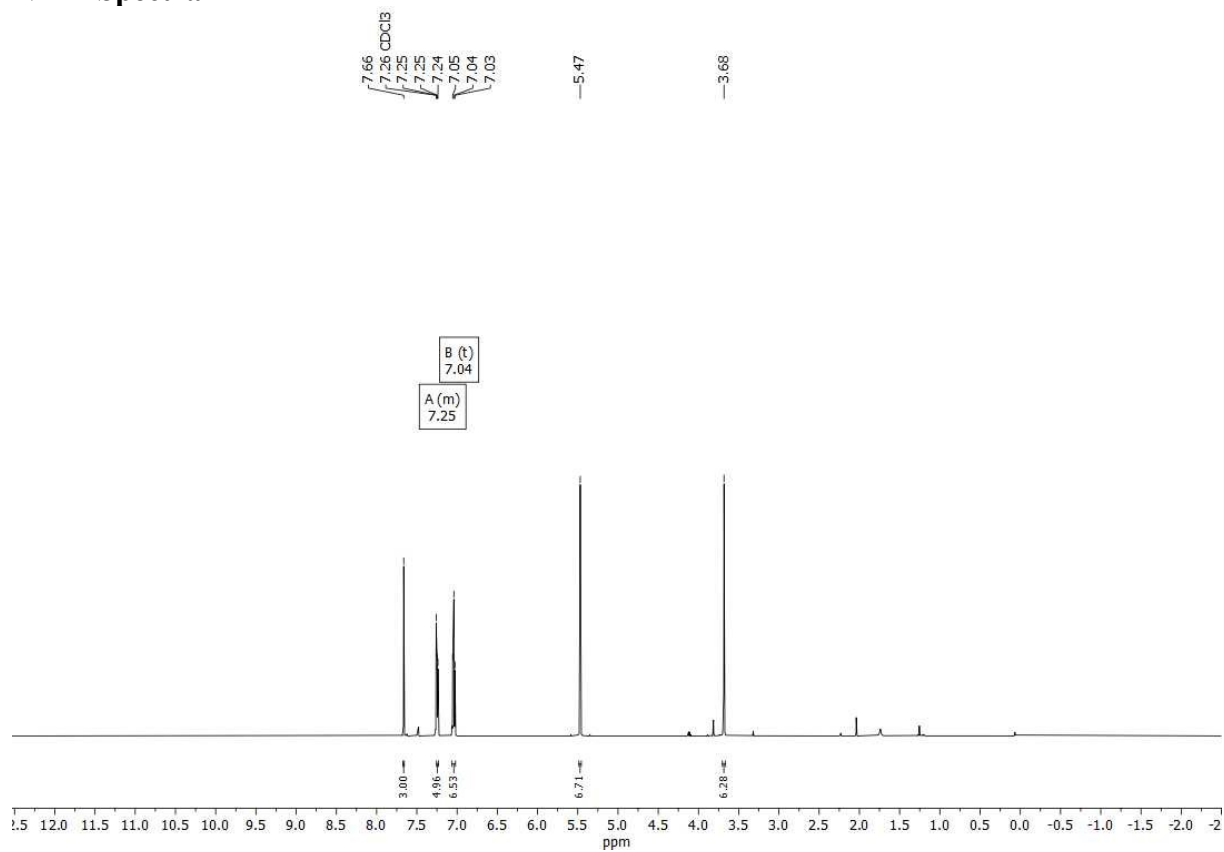


Figure S 11: <sup>1</sup>H NMR of TFTA in CDCl<sub>3</sub>.

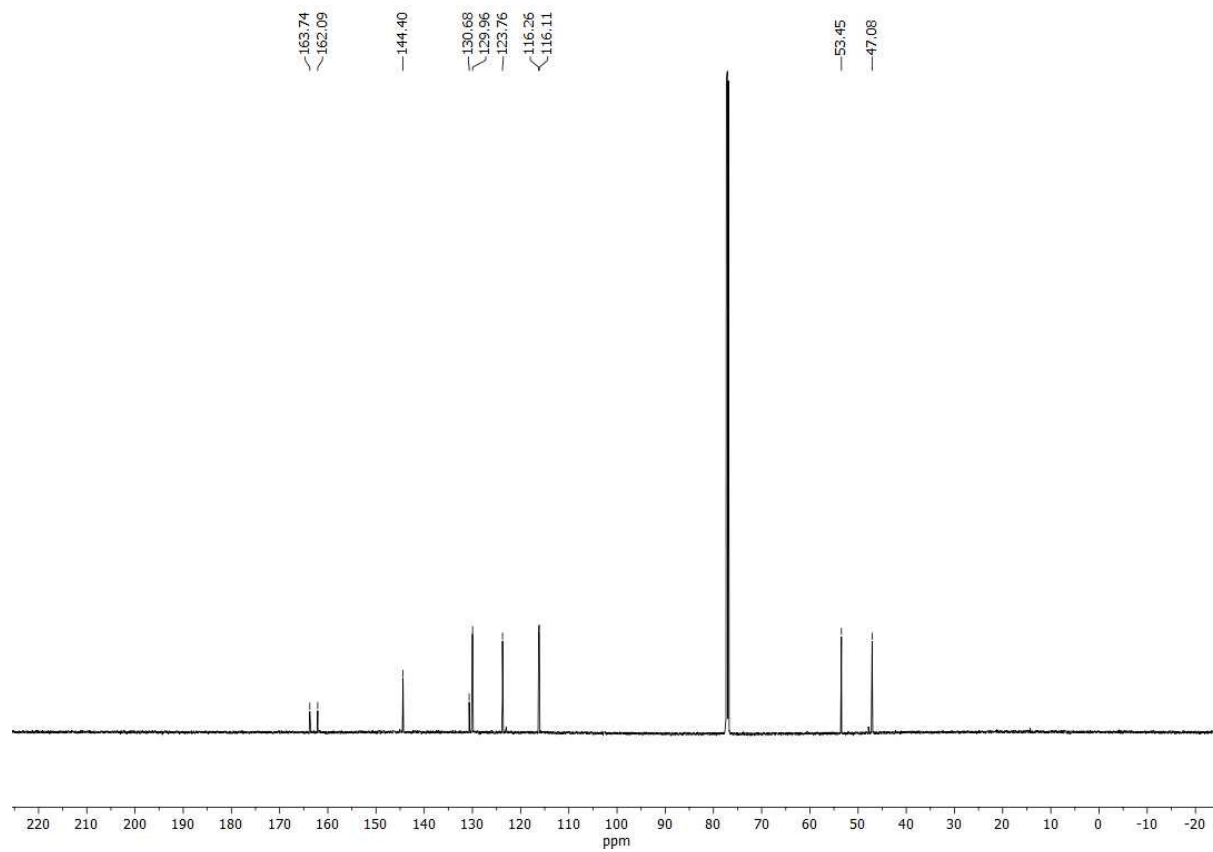


Figure S 12: <sup>13</sup>C NMR of TFTA in CDCl<sub>3</sub>.

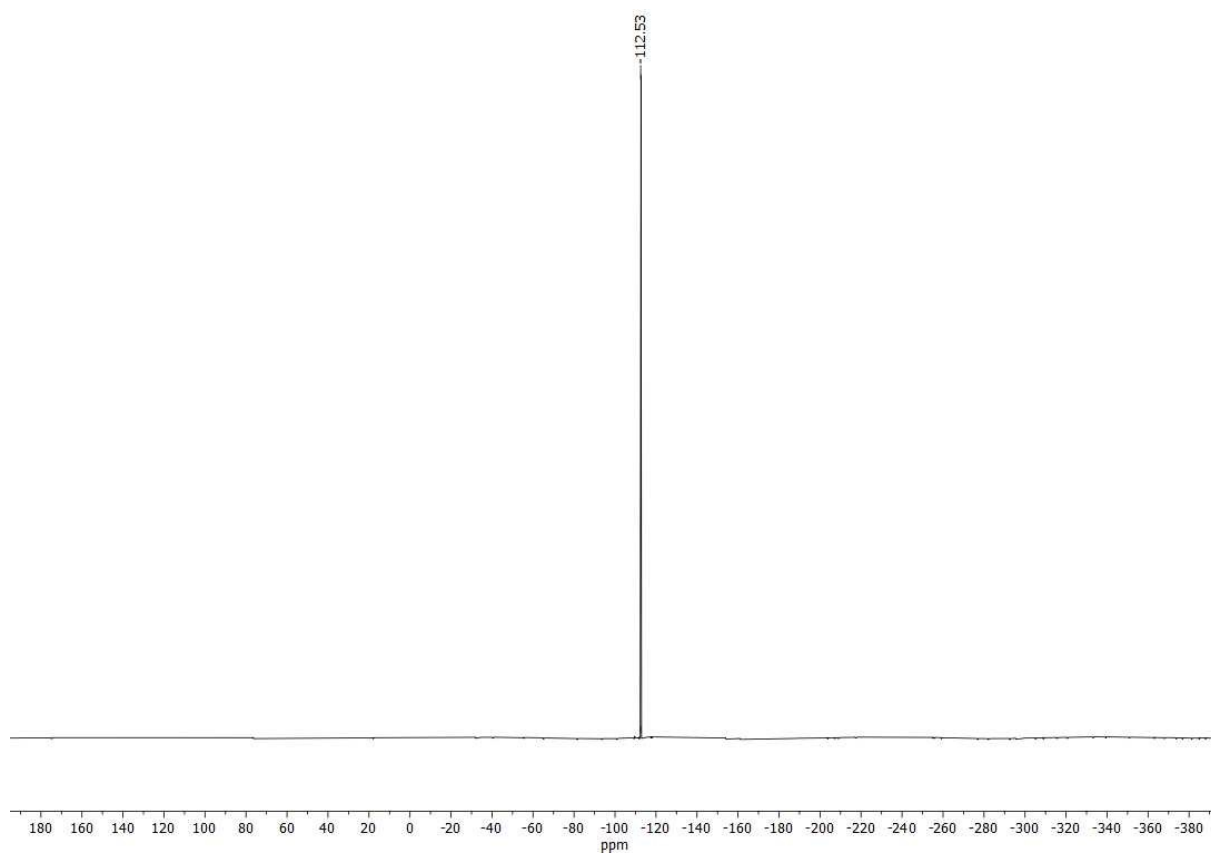


Figure S 13:  $^{19}\text{F}$  NMR of TFTA in  $\text{CDCl}_3$ .

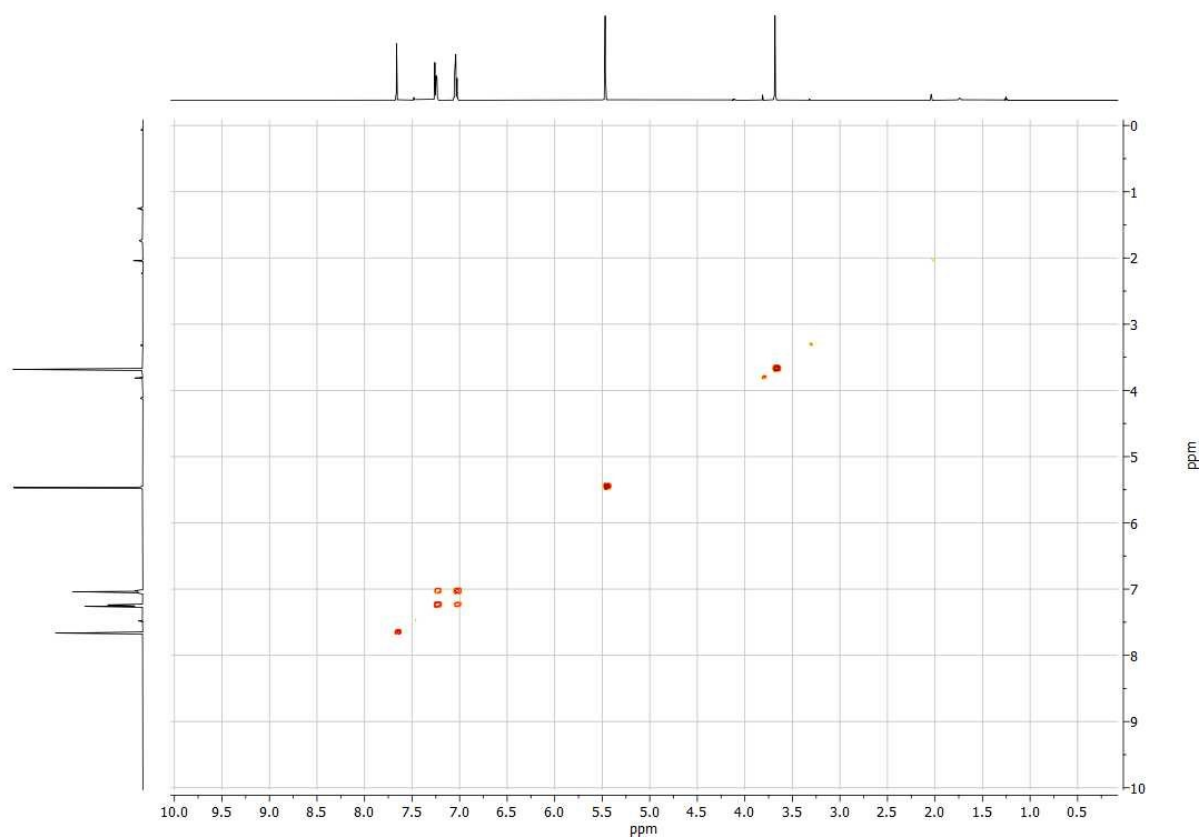


Figure S 14:  $^1\text{H}$   $^1\text{H}$  Cosy NMR of TFTA in  $\text{CDCl}_3$ .

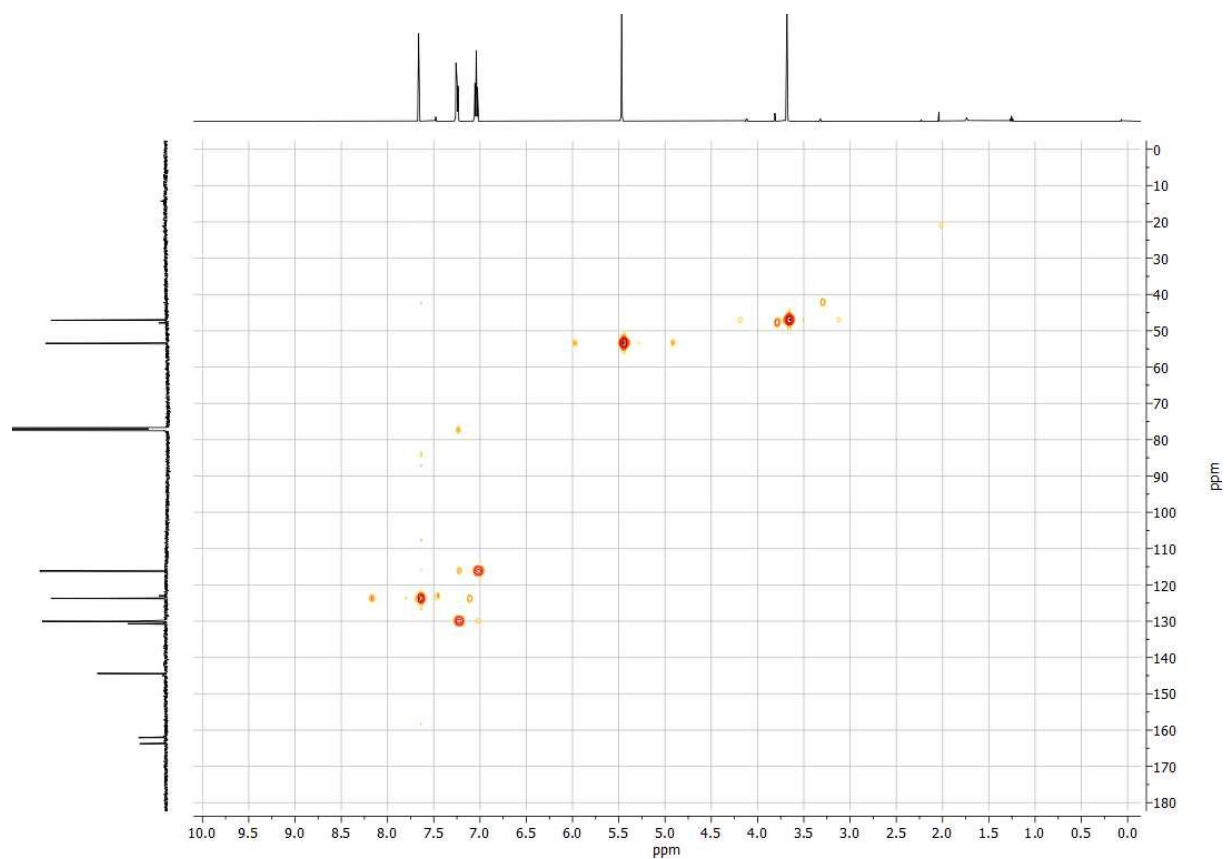


Figure S 15:  $^1\text{H}$   $^{13}\text{C}$  HMBC NMR of TFTA in  $\text{CDCl}_3$ .

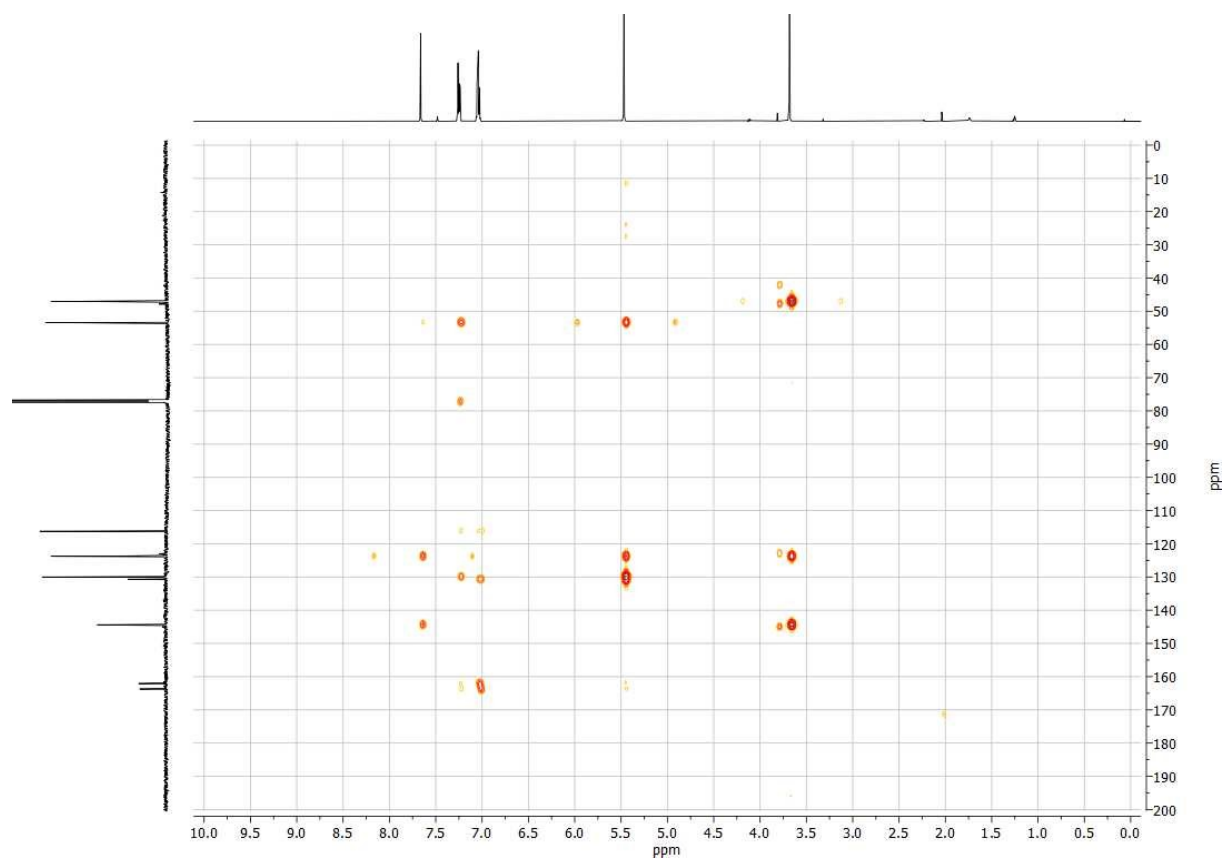


Figure S 16:  $^1\text{H}$   $^{13}\text{C}$  HMQC NMR of TFTA in  $\text{CDCl}_3$ .